J Mater Sci (2013) 48:4758–4765
DOI 10.1007/s10853-013-7266-0

NANOSTRUCTURED MATERIALS

# Phase transformations in Al–Mg–Zn alloys during high pressure torsion and subsequent heating

**O. A. Kogtenkova · A. A. Mazilkin · B. B. Straumal · G. E. Abrosimova · P. Zięba · T. Czeppe · B. Baretzky · R. Z. Valiev**

Received: 12 November 2012 / Accepted: 21 February 2013 / Published online: 2 March 2013


**Abstract** The structure, phase composition, and their thermal evolution were studied in case of ternary Al–Zn–Mg alloys before and after high-pressure torsion (HPT) in Bridgman anvils. The as-cast non-deformed alloys contained the fine particles of $Mg_{32}(Al,Zn)_{49}$ (τ phase), $MgZn_2$ (η phase), $AlMg_4Zn_{11}$ (η′ phase), and $Mg_7Zn_3$ phases embedded in the matrix of Al-based solid solution. During heating in differential scanning calorimeter (DSC), all these phases dissolved around 148 °C. The τ nanoparticles coherent with (Al) matrix-formed instead around 222 °C. HPT of the as-cast alloys strongly refined the grains of (Al) solid solution from 500 μm to 120–150 nm. The particles of τ, η, η′, and $Mg_7Zn_3$ phases fully dissolved in the (Al) matrix. During the following DSC-heating, particles of η phase appeared and grew. Their amount became maximal around 166 °C. The growth of η phase in the fine-grained HPT-treated alloys instead of τ phase in the coarse-grained ones is explained by the shift of the (Al) + η/(Al) + η + τ/(Al) + τ lines in the Al–Zn–Mg ternary phase diagram due to the grain boundary (GB) adsorption. At 166 °C the η phase formed the continuous flat layers in numerous (Al)/(Al) GBs. This corresponds to the complete GB wetting by the η phase. Other (Al)/(Al) GBs contain separated lenticular η particles (incomplete GB wetting). Increasing the temperature from 166 to 320 °C led to the disappearance of the completely wetted (Al)/(Al) GBs. In other words, the transition from complete to the incomplete wetting of (Al)/(Al) GBs by the η phase proceeds between 166 °C and 320 °C.

O. A. Kogtenkova · A. A. Mazilkin · B. B. Straumal · G. E. Abrosimova
Institute of Solid State Physics, Russian Academy of Sciences, Ac. Ossipyan str. 2, 142432 Chernogolovka, Russia

A. A. Mazilkin · B. B. Straumal · B. Baretzky
Karlsruher Institut für Technologie (KIT), Institut für Nanotechnologie, Hermann-von-Helmholtz-Platz 1, 76344 Eggenstein-Leopoldshafen, Germany

B. B. Straumal (✉)
Moscow Institute of Physics and Technology (State University), Institutskii per. 9, 141700 Dolgoprudny, Russia
e-mail: straumal@issp.ac.ru; straumal@mf.mpg.de

P. Zięba · T. Czeppe
Institute of Metallurgy and Materials Science, Polish Academy of Sciences, Reymonta St. 25, 30-059 Cracow, Poland

R. Z. Valiev
Ufa State Aviation Technical University, K. Marx str. 12, 450000 Ufa, Russia

## Introduction

Al–Zn–Mg alloys play an important role in the technology of light alloys because of their good combination of strength and ductility [1]. Further improvement of the mechanical properties of Al–Zn–Mg alloys is possible by tailoring their microstructure, particularly using the combination of severe plastic deformation (SPD) and following heat treatment [2, 3]. Different variants of SPD such as equal-channel angular pressing (ECAP) [3], high pressure torsion (HPT) [4], cryorolling [5], stir friction processing [6], etc., permit to change the composition of Al-matrix, as well as morphology, spectrum and stoichiometry of strengthening precipitates [5, 7]. In order to investigate the phase transformations in Al–Mg–Zn alloys during high pressure torsion and subsequent heating we have chosen the Al–5 wt% Zn–2 wt%Mg and Al–10 wt% Zn–4 wt%Mg alloys (further called as Al–5Zn–2Mg and Al–10Zn–4Mg). We

previously studied the strengthening/softening processes under HPT as well as grain boundary (GB) wetting phenomena in these alloys [8]. In order to characterize the kinetics of phase transformations we used the differential scanning calorimetry (DSC) being a very powerful method for the characterization of SPD-treated alloys [9].

## Experimental methods

Al–5Zn–2Mg and Al–10Zn–4Mg alloys were prepared from high-purity components (99.9995 % Al, 99.999 % Zn, and 99.995 % Mg) by vacuum induction melting and casting into 10 mm diameter rods. The 0.6 mm thick as-cast disks of these alloys obtained after grinding, sawing and chemical etching were subjected to HPT at room temperature under the pressure of 5 GPa in a Bridgman anvil type unit (5 torsions, 1 rpm). The as-cast and HPT-treated samples were studied with use of the DSC TA Instruments calorimeter (model Q1000) in dry helium, at cooling and heating rates of 10 K/min. In order to record the DSC curves, the samples were heated from −10 to 320 °C. Transmission electron microscopy (TEM) investigations were carried out using a TECNAI FEI, G2 FEG microscope at an accelerating voltage of 200 kV. Scanning electron microscopy (SEM) investigations were carried out on a Philips XL30 scanning microscope equipped with a LINK ISIS energy-dispersive spectrometer produced by Oxford Instruments. X-ray diffraction (XRD) data were obtained on a Siemens diffractometer (Co Kα radiation). Grain size was estimated by the XRD line broadening using the Scherer formula [10].

## Results

The Al–5Zn–2Mg and Al–10Zn–4Mg coarse-grained alloys (as cast state prior to HPT deformation) contained the fine particles of $Mg_{32}(Al,Zn)_{49}$ (τ phase), $MgZn_2$ (η phase), $AlMg_4Zn_{11}$ (η′ phase), and $Mg_7Zn_3$ phases embedded in the matrix of Al-based solid solution (Fig. 1a, lower curve). The (Al) matrix was coarse-grained with grain size of 500 μm. The intermetallic $Mg_{32}(Al,Zn)_{49}$ τ phase formed colonies of nanoparticles (Fig. 2a). Colony size was about 500 nm. The dislocation density in (Al) was $\sim 10^{12}$ $m^{-2}$. XRD (Fig. 1a) clearly reveals the presence of τ, η, $Mg_7Zn_3$, and η′ phases in the Al–10Zn–4Mg alloy but only traces of the minor phases in the Al–5Zn–2Mg alloy. This means that their volume fraction in the Al–5Zn–2Mg alloy is less than 1 %.

The microstructure of the Al–Zn–Mg alloys after HPT deformation (Fig. 2b) exhibited (Al) grains with the mean size of 150 nm (Al–5Zn–2Mg) and 120 nm (Al–10Zn–4Mg).

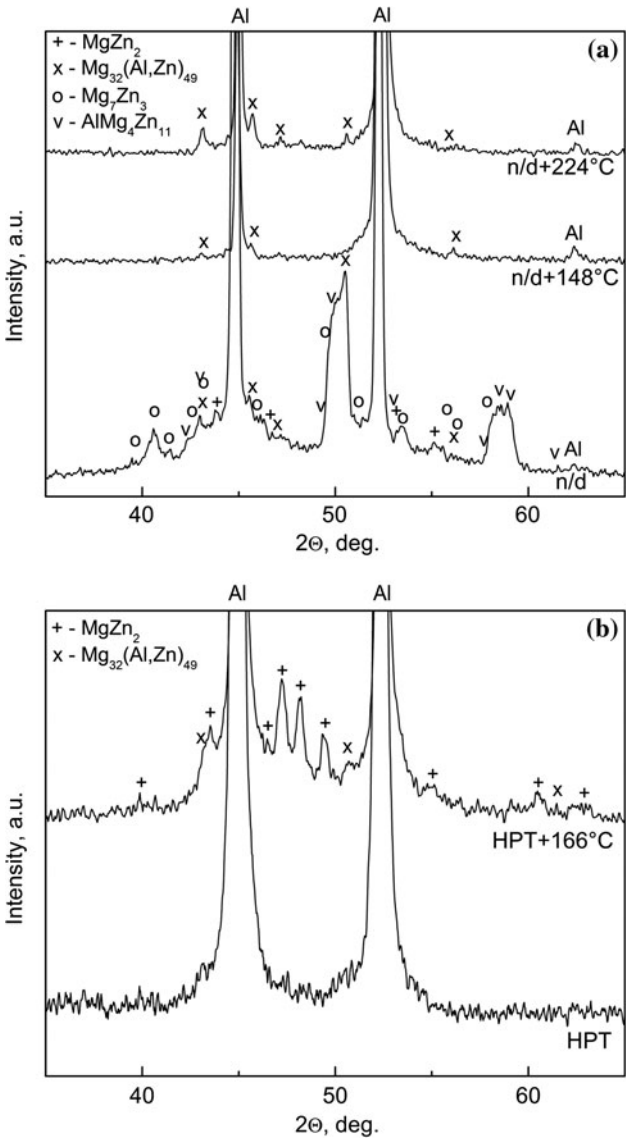


**Fig. 1** X-rays diffraction curves for the Al–10Zn–4Mg alloy, the peaks from $Mg_{32}(Al,Zn)_{49}$ (τ phase), $MgZn_2$ (η phase), $AlMg_4Zn_{11}$ (η′ phase), $Mg_7Zn_3$ phase, and Al solid solution marked by different symbols: **a** lowest curve marked *n/d*—non-deformed, coarse-grained sample; middle curve, *n/d* + 148 °C—after heating up to 148 °C in DSC; *upper curve*, *n/d* + 224 °C after heating up to 224 °C. **b** The sample after HPT *lower curve*, after HPT and heating up to 166 °C in DSC *upper curve*

Dislocations have been observed to be mainly arranged in subgrain boundaries. XRD and TEM did not detect the secondary phases. It means that HPT led not only to the strong grain refinement in the (Al)-matrix but also to the full dissolution of all fine particles of τ, η, η′, and $Mg_7Zn_3$ phases.

In Fig. 3, the temperature dependences of heat flow (DSC curve) is shown for the as-cast Al–5Zn–2Mg (Fig. 3a) and Al–10Zn–4Mg (Fig. 3b) alloys heated from −10 to 320 °C with the rate of 10 K/min. During the

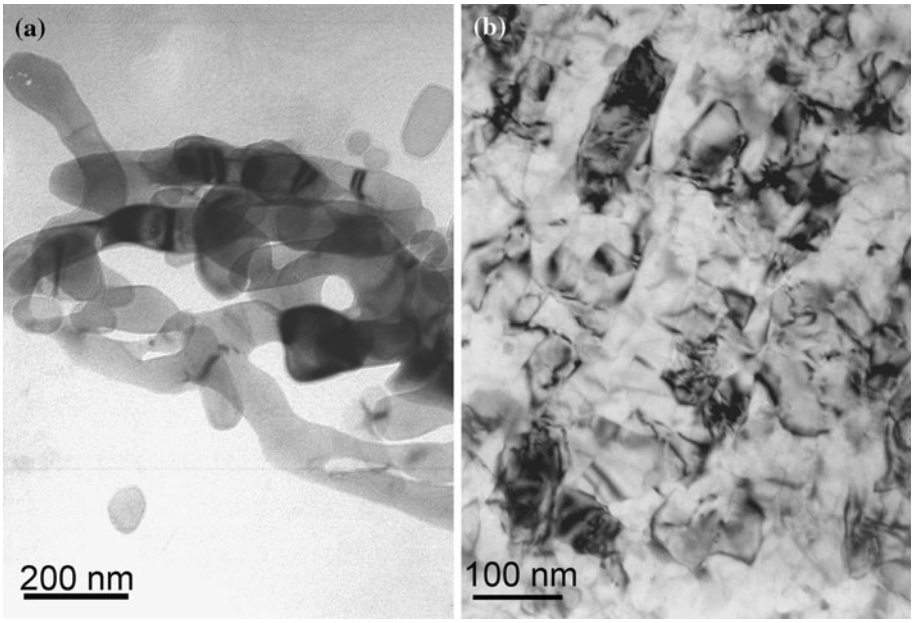


**Fig. 2** Bright-field TEM micrographs of the Al–10Zn–4Mg alloy. **a** As-cast coarse-grained state, colony of $Mg_{32}(Al, Zn)_{49}$ ($\tau$ phase) nanoparticles embedded in the (Al) matrix. **b** Fine-grained sample after HPT deformation

heating an endothermic reaction took place. According to the standard approach to the quantification of the DSC curves of the multiphase alloys [11] (the procedure also included to the quantification software of the modern DSC equipment), the reaction starts at the onset point and the temperature of the end of reaction may be estimated from the intersection of a tangent with the base line, neglecting the thermal lag. In the case of Al–5Zn–2Mg alloy (Fig. 3a) the endothermic reaction started below the onset point (107.0 °C) at about 80 °C and finished at about 185 °C. Its integral heat effect was 1.55 J/g (for comparison, the melting enthalpy in the Al-based alloys is about 200 times higher [12]). Similar reaction in the Al–10Zn–4Mg alloy started at 91.4 °C and finished at 148.3 °C (Fig. 3b). Its integral heat effect was 7.22 J/g. The endothermic reactions in the Al–Zn–Mg alloys are usually connected with dissolution of strengthening precipitates [5, 9, 13].

Two samples of the Al–5Zn–2Mg and Al–10Zn–4Mg alloys were prepared for the TEM examination by heating in the DSC up to 146 and 148 °C, respectively, and immediately cooled down. The TEM and XRD (Fig. 2a, middle curve) data reveal that almost all minor $\eta$, $\eta'$ and $Mg_7Zn_3$ phases have disappeared. Only very weak peaks of $\tau$ phase are still presented. They are visible also in TEM micrographs (Fig. 4). It means that the endothermic peaks in the DSC curves (Fig. 3) correspond to the full dissolution of the $\eta$, $\eta'$ and $Mg_7Zn_3$ phases and partial dissolution of $\tau$ phase. The difference of the endothermic heat effects (Fig. 3a, b) shows that the amount of minor phases in the as-cast Al–10Zn–4Mg alloy is about eight times higher than in the Al–5Zn–2Mg alloy. This fact qualitatively explains the difference in the minor phases XRD-peaks

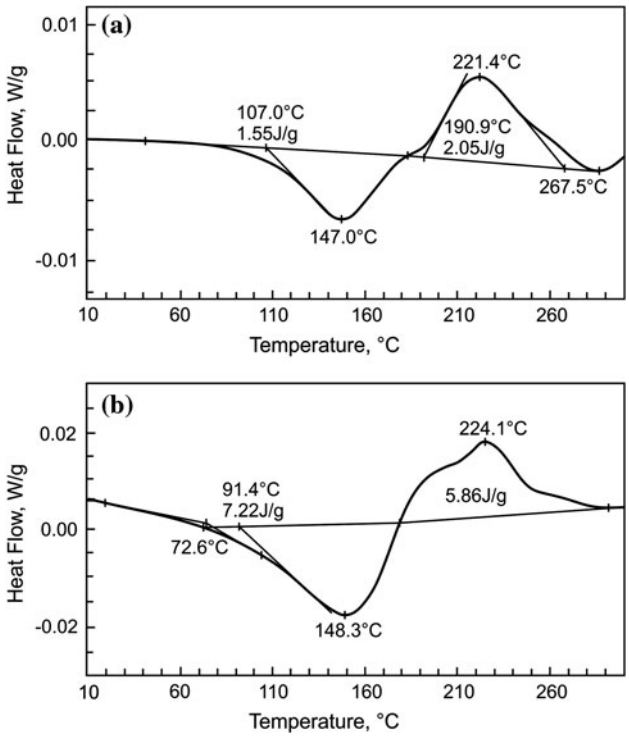


**Fig. 3** DSC curves for the as-cast, coarse-grained samples of alloys: **a** Al–5Zn–2Mg and **b** Al–10Zn–4Mg heated from −10 to 320 °C with the rate of 10 K/min

intensity for the as-cast Al–5Zn–2Mg and Al–10Zn–4Mg alloys.

During the further heating of both as-cast alloys the exothermic reaction took place. It started at 190.9 °C (defined by the onset point) and finished at 267.5 °C in the Al–5Zn–2Mg alloy (Fig. 3a). Its integral heat effect was

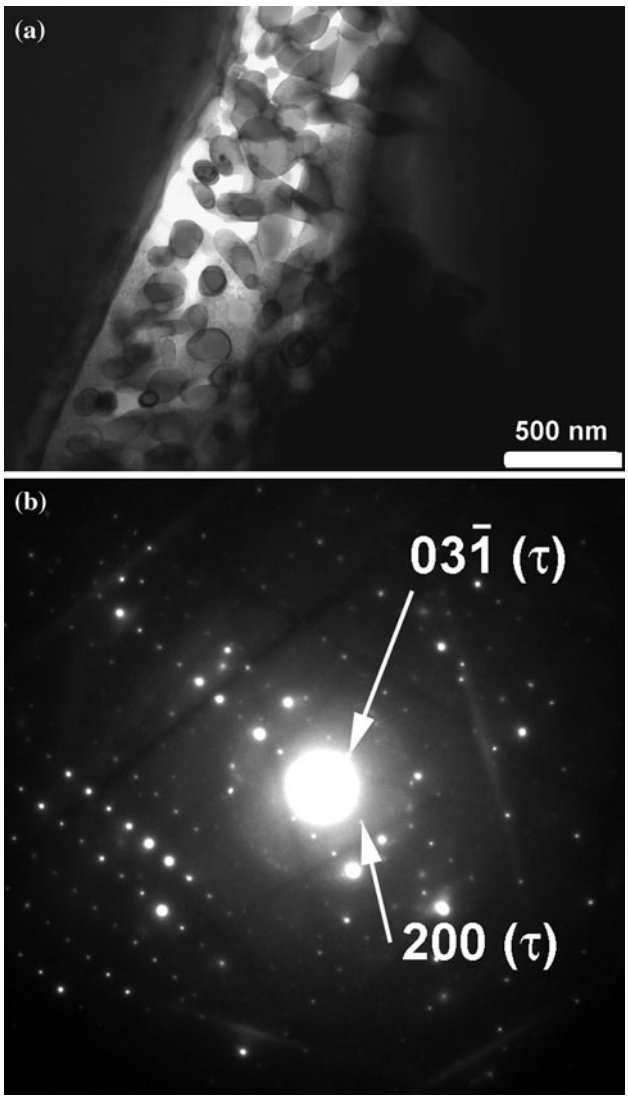


**Fig. 4** Bright-field TEM micrograph of the Al–5Zn–2Mg as-cast alloy heated up to 146 °C (**a**) and respective electron diffraction pattern (**b**). The brightest reflections belong to the Al solid solution grain. The weak reflections belong to the τ phase

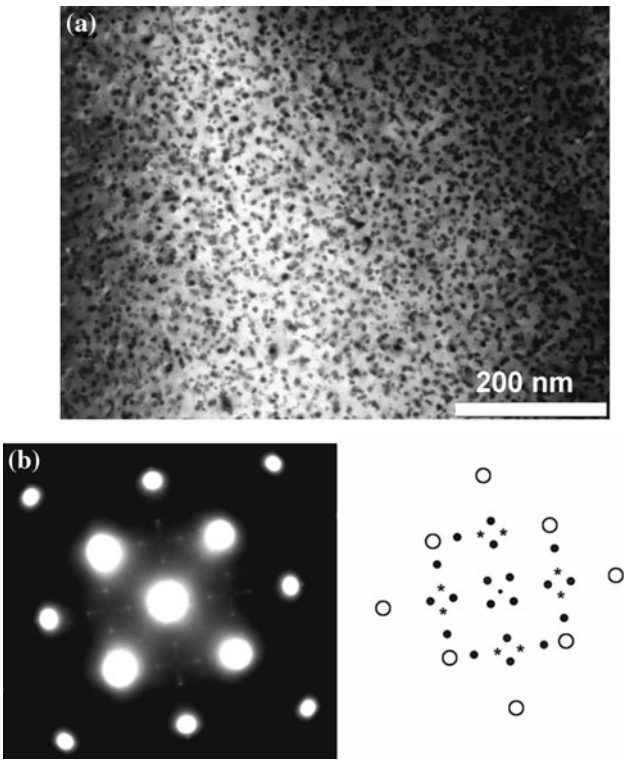


**Fig. 5** Bright-field TEM micrograph of the Al–5Zn–2Mg as-cast alloy DSC-heated up to 222 °C (**a**) and respective electron diffraction pattern (**b**). The brightest reflections belong to the (Al) grain. The weak reflections belong to the τ phase coherent with (Al) matrix. The *scheme* shows the simulated diffraction pattern of the (Al) matrix and the τ-phase. *Open circles* denote the reflections from (Al). *Filled circles* and *stars* correspond to the τ phase, where *circles* denote the reflections with a higher intensity, and those with lower intensity are indicated by the *stars*. Discrepancies with the predicted relative intensities of the reflections are probably due to the local diffraction conditions

2.05 J/g. Similar reaction in the Al–10Zn–4Mg alloy started around 180 °C and finished at 224.1 °C (Fig. 3b). Its integral heat effect was 5.9 J/g. It should be noted, however, that the exothermic reaction in the last case reveal a complex character and doubles. The exothermic reactions in the Al–Zn–Mg alloys are usually connected with precipitation of strengthening particles [5, 9, 13].

Two samples of the Al–5Zn–2Mg and Al–10Zn–4Mg alloys for TEM were as previously prepared by heating in DSC up to 222 and 224 °C, respectively, and cooled down with high rate. The TEM (Fig. 5) and XRD (Fig. 2a, upper curve) data reveal that the samples contain the extremely fine $Mg_{32}(Al,Zn)_{49}$ nanoparticles (τ phase) which are coherent with the (Al) matrix (Fig. 5). It means that the exothermic peaks in the DSC curves (Fig. 3a, b) correspond to the formation of the multiple nanoparticles of η phase. The difference of the exothermic heat effects (Fig. 3) shows that the amount of η phase precipitated in the Al–10Zn–4Mg alloy is about two times higher than in the Al–5Zn–2Mg alloy. This fact qualitatively explains the difference in the XRD-peaks intensity for the η phase in the Al–5Zn–2Mg and Al–10Zn–4Mg alloys.

In Fig. 6, the temperature dependences of the heat flows (DSC curves) are shown for the HPT-treated Al–5Zn–2Mg (Fig. 6a) and Al–10Zn–4Mg (Fig. 6b) alloys subsequently heated from –10 to 320 °C at the rate of 10 K/min. During heating only the exothermic reactions took place. They started at 94.5 °C (onset point temperature 126.8 °C) and finished at 234.6 °C in the Al–5Zn–2Mg alloy with the integral heat effect 16.3 J/g (Fig. 6a). The similar reaction in the Al–10Zn–4Mg alloy started at 96.3 °C (onset point temperature was 122.0 °C) and finished at 206.7 °C (Fig. 6b). Its integral heat effect was 23.5 J/g.

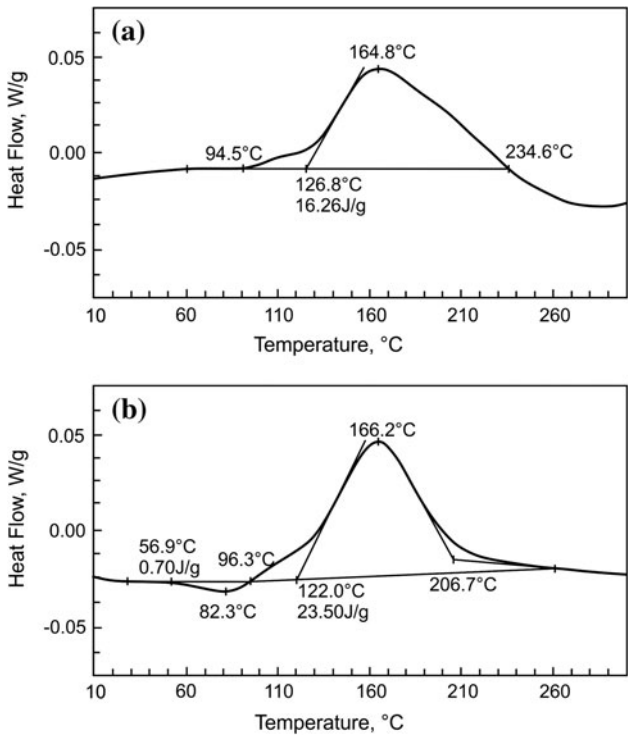


**Fig. 6** DSC curves for the HPT-treated alloys: **a** Al–5Zn–2Mg and **b** Al–10Zn–4Mg, heated from –10 to 320 °C with the rate of 10 K/min

As previously the samples of the HPT-treated Al–5Zn–2Mg and Al–10Zn–4Mg alloys for the TEM analysis were heated in the DSC up to 165 °C and cooled down. The TEM (Fig. 7) and XRD (Fig. 2b) data revealed that the samples contain the fine particles of the $MgZn_2$ η phase. It means that the exothermic peak in the DSC curves (Fig. 6) refers to the formation of the η phase, in analogy to the exothermic effects in Fig. 3, corresponding to the precipitation of the τ phase. The difference of the exothermic heat effects (Fig. 6) suggests that the amount of η phase precipitated in the HPT-treated Al–10Zn–4Mg alloy is about 1.5 times higher than in the Al–5Zn–2Mg alloy.

The TEM micrograph (Fig. 7a) revealed that the η phase precipitated mainly at the grain boundaries of (Al) matrix. The η precipitates in GBs have either the shape of flat continuous plates between adjacent (Al) grains (point A in Fig. 7a) or the lenticular shape (point B in Fig. 7a). Case A corresponds to the complete wetting of (Al)/(Al) GBs by a second solid η phase (like in Al–Mg, Al–Zn, Cu–In, or Co–Cu systems [8, 12, 14]). Case B corresponds to the incomplete wetting of (Al)/(Al) GBs by the second solid phase η [8, 11, 13].

The TEM micrograph in Fig. 7c shows the HPT-treated Al–5Zn–2Mg alloy heated in the DSC up to 320 °C and cooled down. Now the (Al)/(Al) GBs completely wetted by the solid η phase are absent. Only the (Al)/(Al) GBs incompletely wetted by this phase are present in the microstructure, revealing lenticular η phase particles like in the point B.

## Discussion

In accordance with the equilibrium Al–Zn–Mg ternary phase diagram, both Al–5Zn–2Mg and Al–10Zn–4Mg alloys at the studied temperature interval from 10 to 300 °C should consist of (Al) solid solution and $Mg_{32}(Al,Zn)_{49}$ (τ) phase [[16] and references therein]. Therefore, even the slight heating of the coarse-grained as-cast alloys in the DSC measurements led to the dissolution of the non-equilibrium η, η′, and $Mg_7Zn_3$ phases. Above 180 °C only the equilibrium τ phase remained in both alloys. However, both compositions lie very close to the line separating two-phase (Al) + τ and three-phase (Al) + τ + η areas in the phase diagram cross-section. Moreover, the area of the coexistence of the three phases (Al) + η + τ is very narrow. Small composition changes for only about 0.2–0.3 wt% causes that the (Al) + η mixture becomes equilibrium instead of the three-phase composition.

The HPT applied to the Al–5Zn–2Mg and Al–10Zn–4Mg alloys led to the expected strong grain refinement in the (Al) matrix from 500 μm to 120–150 nm, similar to that observed after severe plastic deformation in other Al–Zn–Mg alloys [4, 17, 18]. HPT deformation resulted also in the full dissolution of the particles of τ, η, η′, and $Mg_7Zn_3$ phases into (Al) matrix. The rate of dissolution was very high, despite of the known fact that the application of high pressure, even without deformation always decreases the diffusivity and grain-boundary mobility [19]. For the studied Al–5Zn–2Mg and Al–10Zn–4Mg alloys the mono-phase solid solution composition is not an equilibrium one at room temperature, but only above ~350 and ~450 °C for the Al–5Zn–2Mg and Al–10Zn–4Mg compositions, respectively, [[16] and references therein]. According to the recently proposed approach, it means that the amount of lattice defects produced by HPT in a steady-state is equivalent to the amount of temperature-induced vacancies at a certain effective temperature $T_{eff}$ [[20] and references therein]. In our case $T_{eff}$ is above ~350 °C for the Al–5Zn–2Mg alloy and above ~450 °C for the Al–10Zn–4Mg alloy.

During heating in DSC of the HPT-treated samples the particles of the η phase appeared and grew, in difference to the coarse-grained counterparts where heating led to the growth of the equilibrium τ phase. Why the non-equlibrium η phase did appear and grow in the case of ultrafine-grained HPT-treated alloys instead of the equilibrium τ phase? Recently it has been observed that the lines of phase equilibrium were shifted in nano-grained oxides [21]

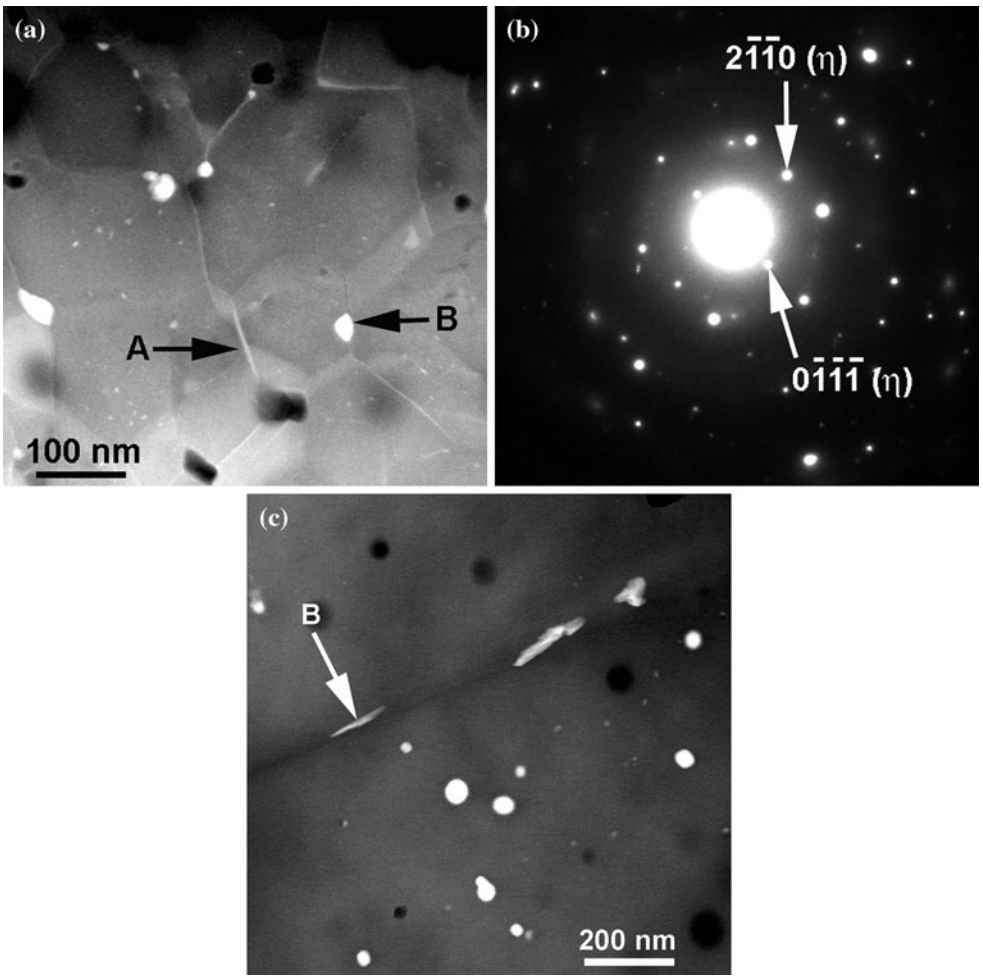


**Fig. 7** Bright-field TEM micrograph of the Al–5Zn–2Mg HPT-treated alloy (**a**) heated in DSC-equipment up to 165 °C. (Al) grains are *dark-grey*, η precipitates are *white*. **b** Respective electron diffraction pattern. The brightest reflections belong to the (Al) grain. The weak reflections belong to the η phase. **c** Same alloy DSC-heated up to 320 °C. *A* (Al)/(Al) GB completely wetted by the η phase. *B* (Al)/(Al) GB incompletely wetted by the η phase

and ultrafine-grained steels [22] in comparison with their coarse-grained counterparts. Due to the strong grain boundary adsorption the average composition of the nano- and ultrafine-grained alloys may be different from the composition of the grains interior. Both alloys studied in this work are very close to the border line of the (Al) + τ two-phase area. In turn, the two-phase areas (Al) + τ and (Al) + η are very close to each other. They are separated with a quite narrow three-phase (Al) + η + τ area, which is only 0.2–0.3 wt% broad. In other words, the additional GBs formed by the HPT absorbed this 0.2–0.3 wt% of solutes atoms and shifted the composition of grains interior from (Al) + τ into (Al) + η phase composition. It has been observed recently in Al–Zn–Mg alloys that Mg strongly segregates to the (Al)/(Al) GBs [23, 24]. On the other hand, the concentration of Zn in the (Al)/(Al) GBs almost coincide with the bulk one [23, 24]. This difference in GB segregation of Zn and Mg atoms can shift the composition of the bulk phases from (Al) + τ into (Al) + η region if the specific area of GBs is high enough. Estimation shown in Fig. 8 demonstrates such a possible shift of bulk composition in case of both studied alloys for the grain sizes of 150 nm. In Fig. 8 open circles show the estimated composition for the grains interior in the case while Al/Al grain boundaries contain one monolayer of adsorbed Mg and the same time Zn GB adsorption is negligible.

The η phase formed above 96 °C grew as the continuous flat layers in some (Al)/(Al) GBs grains (complete GB wetting). The GB wetting by the melt was observed in the Al–5Zn–2Mg and Al–10Zn–4Mg alloys earlier [14]. The GB wetting by a second liquid or solid phase also was observed in the binary Al–Zn and Al–Mg alloys [8, 12, 15]. This phenomenon is very important in processes such as liquid phase sintering, brazing, welding, or melt infiltration [[25] and references therein]. It was carefully investigated

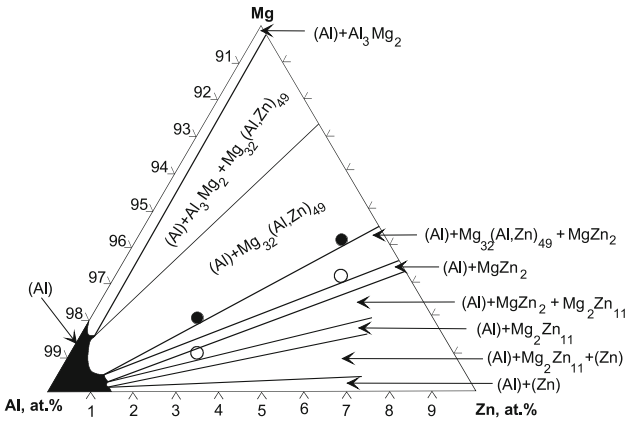


**Fig. 8** The Al-rich corner of the Al–Mg–Zn ternary phase diagram at 25 °C [16]. *Filled circles* mark the composition of the studied alloys. *Open circles* show the estimated composition for the grains interior in case of the monolayer Mg grain-boundary adsorption while Zn GB adsorption is absent and for the grain size of 150 nm

for many years [[26] and references therein]. The GB is completely wetted if the contact angle $\theta$ between the GB and melt is zero ($\theta = 0°$). In this case, the GB separating the grains is completely substituted by the liquid phase. The GB is incompletely wetted if the contact angle between the GB and melt is $\theta > 0°$. In this case, the GB can exist in the equilibrium contact with the liquid phase. The transition from incomplete to complete GB wetting proceeds with increasing temperature [14, 15]. This occurs at a certain temperature $T_w$ if the energy of two solid–liquid interfaces $2\sigma_{SL}$ becomes lower than the GB energy, $\sigma_{GB} > 2\sigma_{SL}$. Cahn [27] and Ebner and Saam [28] first showed that the (reversible) transition from incomplete to complete wetting can proceed with increasing temperature, and that it is a true surface transformation. Later, such transitions were observed in numerous experiments [14, 15]. The wetting phase can be as well liquid [14, 15] as solid [29].

At 224 °C all GB the layers of η phase appeared to be broken into the separated lenticular particles. In other words, the transition from complete to the incomplete wetting of (Al) GBs by the η phase proceeds between 166 and 224 °C. At temperature 166 °C both completely and incompletely wetted GBs are present in the samples since the transition from incomplete to complete wetting may proceed at different temperatures for the GBs with different energies and the energies of GBs and interphase boundaries drastically depend on their crystallographic parameters [30].

## Summary and conclusions

The phase transformations in two Al–Mg–Zn alloys were studied in as cast samples and resulting from the high pressure torsion and subsequent heating. HPT led to the full dissolution of small particles of τ, η, η′, and $Mg_7Zn_3$ phases embedded in the matrix of Al-based solid solution. Such named effective temperature of HPT in this system was above 350–450 °C. During the heating of the as-cast samples, the non-equilibrium η, η′ and $Mg_7Zn_3$ phases dissolved while the equilibrium τ phase grew. On the other hand, the heating of the nanograined Al solid solution formed by HPT led to the formation of the η phase which grew with the increasing temperature. It was observed that Mg strongly segregates to the (Al)/(Al) grain boundaries while Zn does not. This GB segregation led to the depletion of Al-grains in Mg in case of nanograined alloys in comparison with the coarse-grained ones. As a result, the composition of the Al solid solution grains interiors shifts from the (Al) + τ into (Al) + η phase equilibrium field of the ternary Al–Mg–Zn phase diagram. In the case of the HPT-treated alloy, above about 95 °C the η phase formed the continuous GB layer separating the Al solid solution grains from each other. At higher temperature of 224 °C, contrary, the η phase had a shape of separated lenticular GB particles. In other words, the transition from the complete to the incomplete GB wetting proceeds between 166 and 224 °C in the case of investigated compositions.

**Acknowledgements** Authors thank the Russian Foundation for Basic Research (contracts 11-03-01198 and 11-08-90439), ERA.Net RUS program (Grant STProjects-219 NanoPhase), program of bilateral cooperation between Russian and Polish Academies of sciences, the grant of President of Russian Federation for young scientists (MK-3748.2011.8) and Polish National Science Centre (Grant UMO-2011/01/M/ST8/07822) for the financial support.

## References

1. Furukawa M, Horita Z, Nemoto M, Valiev RZ, Langdon TG (1996) Acta Mater 44:4619
2. Roven HJ, Liu M, Murashkin MY, Valiev RZ, Kilmametov AR, Ungár T, Balogh L (2008) Mater Sci Forum 604:179
3. Cepeda-Jimenez CM, Garcia-Infanta JM, Rauch EF, Blandin JJ, Ruano OA, Carreno F (2012) Metal Mater Trans A 43:4224
4. Garcia-Infanta JM, Zhilyaev AP, Sharafutdinov A, Ruano OA, Carreno F (2009) J Alloys Comp 473:163
5. Krishna KG, Sivaprasad K, Venkateswarlu K, Kumar KCH (2012) Mater Sci Eng A 535:129
6. Liu FC, Ma ZY (2008) Scr Mater 58:667
7. Sha G, Wang YB, Liao XZ, Duan ZC, Ringer SP, Langdon TG (2009) Acta Mater 57:3123
8. Straumal B, Valiev R, Kogtenkova O, Zieba P, Czeppe T, Bielanska E, Faryna M (2008) Acta Mater 56:6123
9. Gao N, Starink MJ, Langdon TG (2009) Mater Sci Technol 25:687
10. Ungar T, Borbely A (1996) Appl Phys Lett 69:3173
11. Dean JA (1995) The analytical chemistry handbook. McGraw Hill, New York, p 151 (Standards ASTM D 3417, ASTM D 3418, ASTM E 1356, ISO 11357)
12. Kogtenkova OA, Protasova SG, Mazilkin AA, Straumal BB, Zięba P, Czeppe T, Baretzky B (2012) J Mater Sci 47:8367. doi: 10.1007/s10853-012-6786-3

13. Gao N, Starink MJ, Furukawa M, Horita Z, Xu C, Langdon TG (2006) Mater Sci Forum 503:275
14. Straumal BB, Gust W (1996) Mater Sci Forum 207:59
15. Straumal BB, Gust W, Watanabe T (1999) Mater Sci Forum 294:411
16. Villars P, Prince A, Okamoto H (eds) (1995) Handbook of ternary alloy phase diagrams, vol 10. ASM International, Metals Park
17. Lu J, Yin JG, He Y, Ding BF (2005) Rare Metal Mater Eng 34:742
18. Malek P, Cieslar M, Islamgaliev RK (2004) J Alloys Comp 378:237
19. Molodov DA, Straumal BB, Shvindlerman LS (1984) Scr Metall 18:207
20. Straumal BB, Gornakova AS, Mazilkin AA, Fabrichnaya OB, Kriegel MJ, Baretzky B, Jiang JZ, Dobatkin SV (2012) Mater Lett 81:225
21. Straumal BB, Mazilkin AA, Protasova SG, Myatiev AA, Straumal PB, Baretzky B (2008) Acta Mater 56:6246
22. Straumal BB, Dobatkin SV, Rodin AO, Protasova SG, Mazilkin AA, Goll D, Baretzky B (2011) Adv Eng Mater 13:463
23. Krishna KG, Sivaprasad K, Venkateswarlu K, Kumar KCH (2012) Mater Sci Eng, A 535:129
24. Sha G, Ringer SP, Duan ZC, Langdon TG (2009) Int J Mater Res 100:1674
25. German RM, Suri P, Park SJ (2009) J Mater Sci 44:1. doi: 10.1007/s10853-008-3008-0
26. Empl D, Felberbaum L, Laporte V, Chatain D, Mortensen A (2009) Acta Mater 57:2527
27. Cahn JW (1977) J Chem Phys 66:3667
28. Ebner C, Saam WF (1977) Phys Rev Lett 38:1486
29. López GA, Mittemeijer EJ, Straumal BB (2004) Acta Mater 52:4537
30. Straumal BB, Klinger LM, Shvindlerman LS (1984) Acta Metall 32:1355